

Journal of
**Micro/Nanolithography,
MEMS, and MOEMS**

Nanolithography.SPIEDigitalLibrary.org

Development of nanoimprint processes for photovoltaic applications

Hubert Hauser
Nico Tucher
Katharina Tokai
Patrick Schneider
Christine Wellens
Anne Volk
Sonja Seitz
Jan Benick
Simon Barke
Frank Dimroth
Claas Müller
Thomas Glinsner
Benedikt Bläsi

Development of nanoimprint processes for photovoltaic applications

Hubert Hauser,^{a,*} Nico Tucher,^a Katharina Tokai,^a Patrick Schneider,^a Christine Wellens,^a Anne Volk,^a Sonja Seitz,^a Jan Benick,^a Simon Barke,^a Frank Dimroth,^a Claas Müller,^b Thomas Glinsner,^c and Benedikt Bläsi^a

^aFraunhofer Institute for Solar Energy Systems ISE, Heidenhofstraße 2, Freiburg 79110, Germany

^bAlbert-Ludwigs-University, IMTEK, Georges-Köhler-Allee 103, Freiburg 79110, Germany

^cEV Group, E. Thallner GmbH, Erich Thallner Street 1, Schärding 4780, Austria

Abstract. Due to its high resolution and applicability for large area patterning, nanoimprint lithography (NIL) is a promising technology for photovoltaic (PV) applications. However, a successful industrial application of NIL processes is only possible if large-area processing on thin, brittle, and potentially rough substrates can be achieved in a high-throughput process. The development of NIL processes using the SmartNIL technology from EV Group with a focus on PV applications is described. The authors applied this tooling to realize a honeycomb texture (8 μm period) on the front side of multicrystalline silicon solar cells, leading to an improvement in optical efficiency of 7% relative and a total efficiency gain of 0.5% absolute compared to the industrial standard texture (isotexture). On the rear side of monocrystalline silicon solar cells, the authors realized diffraction gratings to make use of light trapping effects. An absorption enhancement of up to 35% absolute at a wavelength of 1100 nm is demonstrated. Furthermore, photolithography was combined with NIL processes to introduce features for metal contacts into honeycomb master structures, which were initially realized using interference lithography. As a final application, the authors investigated the realization of very fine contact fingers with prismatic shape in order to minimize reflection losses. © The Authors. Published by SPIE under a Creative Commons Attribution 3.0 Unported License. Distribution or reproduction of this work in whole or in part requires full attribution of the original publication, including its DOI. [DOI: 10.1117/1.JMM.14.3.031210]

Keywords: nanoimprint lithography; solar cells; light trapping; photon management; plasma etching.

Paper 15071SSP received Apr. 28, 2015; accepted for publication Jul. 2, 2015; published online Jul. 29, 2015.

1 Introduction

Measures to maximize absorption of sunlight are continually refined in order to improve solar cell efficiencies.¹ Besides antireflection coatings (ARCs) based on thin-film interference, front side texturing is a standard process in silicon solar cell fabrication. This texturing not only reduces the reflectivity at the front interface, but also leads to a path length enhancement by deflecting the incoming light within the semiconductor. The latter effect gains in importance when looking at silicon wafer-based solar cells becoming thinner and thinner. Silicon as an indirect semiconductor absorbs light close to the bandgap energy only weakly; therefore, an enhanced optical thickness helps to increase the total absorption. Current research trends toward solar cells made of crystalline silicon foils highlight the necessity of finding suitable processes, which are capable of realizing very fine patterns on large areas.^{2,3}

Industrially applied standard processes to realize surface textures in silicon solar cells are based on maskless alkaline⁴ or acidic⁵ etching for mono- and multicrystalline materials, respectively. While stochastically distributed pyramidal textures, as a result of the anisotropic etching in alkaline solutions, already lead to good optical properties, for the isotropic acidic etching on multicrystalline silicon there is considerable room for optimization. Using the so-called

honeycomb texture, a hexagonal array of etching pits realized using lithographic methods, for the first time efficiencies exceeding 20% were reached.⁶ A completely different method to enhance optical thicknesses was suggested by Morf et al. It is based on diffractive elements located on the rear side of the solar cell.⁷

The scope within this work is placed on nanoimprint lithography (NIL) for photovoltaic (PV) applications. This target application implies several technological requirements: typical wafer sizes are $156 \times 156 \text{ mm}^2$ with standard thicknesses well below 200 μm , which are projected to reach values as low as 100 μm until 2020.⁸ Furthermore, substrates are brittle and, especially in the case of multicrystalline silicon, show a considerable roughness. For NIL, this means that the adaptability of stamps to substrates and especially the demoulding process is challenging. To meet these requirements, a Roller-NIL tooling intended for in-line high-throughput processing was developed and tested at Fraunhofer ISE.⁹ The current study investigates the SmartNIL technology, as developed by EV Group. This technology is based on a UV-assisted NIL process using soft stamp materials. The requirements of PV applications were already addressed in the design stage of the SmartNIL technology and were refined in a redesigning step. Furthermore, the high-definition tooling integrated into an EVG6200 mask aligner provides further opportunities concerning precision, alignment steps, and combined processes. Using this tooling, etching masks were made for the honeycomb texturing of multicrystalline silicon and for the fabrication of diffractive gratings

*Address all correspondence to: Hubert Hauser, E-mail: hubert.hauser@ise.fraunhofer.de

on the rear side of monocrystalline silicon solar cells. In both cases, the periodic patterns were applied on the full wafer area. In a next step, the authors tried to tap the full potential of combining different lithographic techniques in order to integrate multiple features into one imprinted pattern. By integrating features for a later metallization grid into the etching mask for the texture pattern, more value can be generated within a single process step. Finally, an approach for realizing very fine contact fingers with a prismatic profile is presented. Thereby, the shading by front contact fingers can be drastically reduced.

2 Methods and Toolings

2.1 Master Origination and Stamp Replication

Interference lithography was applied as the mastering technology. This technology allows for the seamless high-resolution origination of surface structures on very large areas up to the square meter scale.¹⁰ A large diversity of patterns can be realized including periodic (1-D, 2-D, and 3-D photonic crystals) and stochastic features (e.g., well-defined isotropic or anisotropic diffuser structures) as well as combinations thereof.¹¹ Minimum feature sizes are determined by the laser wavelength. An argon-ion laser emitting at 363.8 nm was used; therefore, minimum periods are in the range of 200 nm. The interference pattern can be analogously transferred into a positive or negative tone photoresist as in photolithography processes. To obtain a durable master structure, the pattern defined in the photoresist can either be transferred into the substrate below (e.g., quartz or silicon) by etching processes, or a metal copy (negative) can be replicated by electroplating. In this work, stamps were either replicated from nickel masters realized via electroplating or directly from photoresist masters.

As stamp material, different types of polydimethylsiloxane (PDMS) materials are used, in order to compensate for uneven or rough surfaces and to be able to pattern large areas.^{12,13} PDMS materials are applied using cast moulding or spin coating on the patterned master and are thermally cured afterward. A primer is used to bond the stamp onto a carrier substrate during the curing process.

2.2 Description of the Smart-Nanoimprint Lithography Technology

The key aspects of the EVG SmartNIL technology are conformal imprinting in a UV-assisted process as well as an automated demoulding process of a soft polymer working stamp from the imprinted substrate. This is essential when aiming for a homogeneous residual layer thickness on large areas and even more for having a controlled and repeatable demoulding process. The latter becomes even more crucial when thinking of very thin silicon substrates. A controlled imprint pressure of up to 1.5 bars is applied during the imprinting processes. The aforementioned use of the flexible polymer working stamp technology lowers the processing cost and addresses one key aspect in nanoimprint lithography, the cost and lifetime of the electroplated negative. Polymer stamps such as PDMS offer low surface adhesion to imprint resists, and thus an easy separation of stamp and cured polymer is possible.

By integrating the SmartNIL tooling (consisting of stamp holder for the polymer working stamps and the chuck

accommodating the substrate) into an EVG alignment system, processes like wedge error compensation and optical alignment of polymer stamp and substrate can be applied. Imprinting resolutions below 20 nm were demonstrated using this technology.¹⁴

3 Experimental Work

3.1 Overview of the Solar Cell Features for Which Nanoimprint Lithography Processes Are Evaluated

In the following, some features in (silicon) solar cells, which are addressed within this work by nanoimprint processes, are briefly introduced. Silicon solar cells are textured on the front side in order to reduce reflectivity and increase their optical thickness. Common sizes for these textures are in the range of approximately 5-10 μm . While for high-efficiency solar cells, photolithography is often applied, in industrial fabrication of silicon solar cells these textures are realized without the use of defined etching masks.

As an alternative, the absorption enhancement introduced by diffraction gratings on the wafer rear was already demonstrated in the laboratory scale. Feature sizes are in the range of 500 nm (periods approximately 1 μm). These measures to increase internal optical pathlengths are gaining in importance for decreasing cell thicknesses, which for wafer-based silicon are already below 200 μm .

Most often, solar cells are contacted from the front and the rear. Front contacts lead to shading effects, which can be minimized by both reducing the width of contact fingers and optimizing the shape of the fingers in a way so that light is redirected onto the active solar cell area. In standard processes, the contacting is realized over the textured area. In high-efficiency solar cells fabricated in the laboratory scale, the contacting is often realized over planarized areas to achieve the best possible defined electrical contact. An overview of these addressed features, and which are the subject

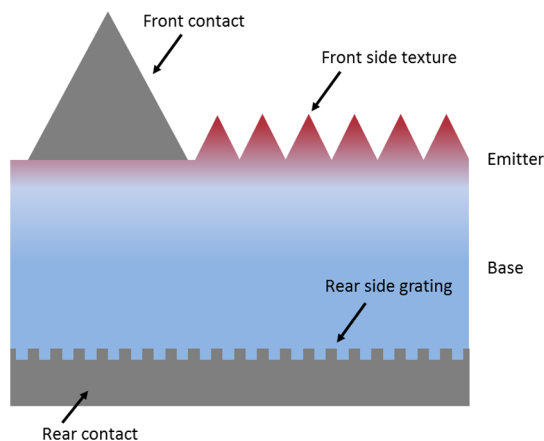


Fig. 1 Rudimentary sketch of a solar cell with features addressed by nanoimprint processes within this work: an ideal prismatic metal contact on a planarized area on the front, a defined micron-scaled front side texture, and a diffractive rear side grating (not to scale). Ideally, the rear side mirror is not patterned to minimize parasitic absorption. A concept to avoid this is based on a aluminium foil-based laser contacting scheme as described in Ref. 15.

of the following subsections, is shown in Fig. 1. Note that it is not necessarily intended that these features have to be combined.

3.2 Honeycomb Texturing of Multicrystalline Silicon

Master structures with the hexagonal pattern of a period of $8\ \mu\text{m}$ were realized using three beams interference lithography on an area of $25 \times 25\ \text{cm}^2$.⁹ Following the electroplating process, stamps made of soft PDMS material were replicated (ELASTOSIL® RT 601 from Wacker, Germany). The structured PDMS layer was around 1 mm thick and was bonded to a polymer backplane for the subsequent NIL process. The NIL process was conducted on $156 \times 156\ \text{mm}^2$ multicrystalline silicon substrates, which represent the industrially applied standard substrate size. Scanning electron microscope (SEM) images showing the imprinted pattern and the very low residual layer are shown in Fig. 2. Following to the NIL process, the pattern defined by the etching mask was transferred into the multicrystalline silicon using plasma etching. The etching processes were conducted on a modified SiNA tool by Piechulla et al.¹⁶ After the plasma etching process, potentially damaged material was removed by a wet chemical treatment. The resulting texture is also shown in Fig. 2. Details on the subsequent solar cell processing as well as the solar cell architecture are given in Ref. 17.

It was found that the optical performance of the honeycomb texture was by far superior compared to the state-of-the-art texture on multicrystalline silicon based on a stochastic etching using an acidic etching solution (the so-called isotexture). It was even superior to the excellent pyramidal textures on monocrystalline silicon. The gain in optical performance led to an enhancement in the short-circuit current density j_{sc} of up to $2.5\ \text{mA}/\text{cm}^2$ (from 35.0 to $37.50\ \text{mA}/\text{cm}^2$) of honeycomb-textured compared to isotextured solar cells on multicrystalline material.¹⁷ This is evidence for a relative increase in optical efficiency of 7%. Furthermore, a gain in overall conversion efficiency of 0.5% absolute was achieved on large area $156 \times 156\ \text{mm}^2$ solar cells using high-throughput pilot line equipment and an aluminum-back surface field (Al-BSF) cell architecture (efficiency of honeycomb-textured cell 17.8%).

3.3 Rear Side Diffraction Gratings

Internal light paths can also be enhanced by diffraction induced by photonic structures on the wafer rear side.⁷ In recent studies, the authors demonstrated for a pitch of $1\ \mu\text{m}$ that crossed gratings outperform linear gratings¹⁸ and that excellent electrical properties of a passivated planar rear can be maintained by etching the grating into an amorphous silicon layer, which is separated from the bulk by a very thin aluminum oxide layer.¹⁹ Both works imprinted the photonic structure on an area of about $5 \times 5\ \text{cm}^2$ on $200\text{-}\mu\text{m}$ thick monocrystalline silicon wafers. Now, the imprint area is enhanced to 100-mm round wafer size using the EVG SmartNIL tooling. As shown in Ref. 19, the benefit of such a photonic structure in particular is pronounced for very thin solar cells. However, especially the demoulding process becomes more and more critical for thin wafers. The authors succeeded in imprinting a crossed grating pattern with $1\text{-}\mu\text{m}$ pitch and about 300-nm pattern depth on full 100-mm round wafers as thin as $50\ \mu\text{m}$ as shown in Fig. 3. An automated sequential demoulding on such thin wafers was successfully demonstrated. Additionally, in Fig. 3, an SEM micrograph of a grating structure etched into silicon as well as a graph showing the measured absorption enhancement induced by such a grating for a $200\text{-}\mu\text{m}$ -thick silicon wafer are compared to a planar reference. The useful absorption enhancement within silicon is extracted from the simulations in Ref. 19. It can be seen that a total absorption enhancement of up to 35% at a wavelength of 1100 nm is achieved. The difference in absorptance for wavelength below $1\ \mu\text{m}$ is a result of the slightly different antireflection coating thicknesses of the samples. Etching processes on these substrates are not in the scope of current work and will therefore be published in future studies. Beyond the results published in this work, a significant quantum efficiency enhancement is demonstrated in the near infrared on the final solar cell level.¹⁵

3.4 Single Step Definition of Texturing Features and Contact Grid Geometry

As discussed earlier, by introducing defined textures the optical performance can be improved. When aiming to introduce an additional process step into the process chain such as the

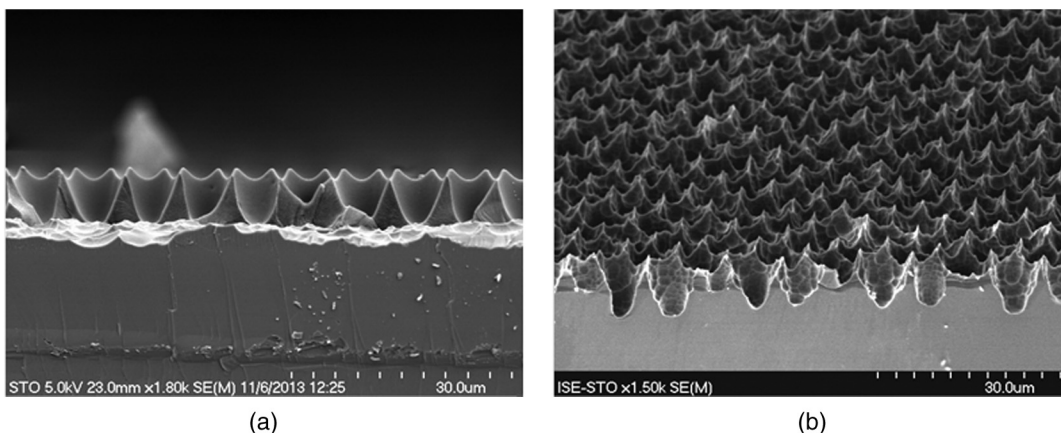


Fig. 2 (a) Scanning electron microscope (SEM) micrographs of the imprinted etching mask and (b) the resulting honeycomb texture. The pattern transfer was realized using plasma etching with a subsequent wet chemical smoothing of the surface.

patterning of etching masks, it is desirable to achieve added value by implementing an additional functionality in the mask layout. As one possibility, features were integrated for a latter contact grid into the template for the honeycomb texturing.

As starting point, the authors used master structures realized with three-beam interference lithography.⁹ The following process chain is schematically visualized in Fig. 4(a) and single process steps are numbered for the sake of clarity. These masters with a hexagonal pattern with a period of 8 μm were then replicated into SU8-2002 from MicroChem, USA in a solvent-assisted embossing process without UV exposure (step 1). After the demoulding (step 2), a photolithography process using a photomask with a contact grid geometry (line widths of 15 μm and a pitch of 800 μm) was realized (step 3). After the following postexposure bake and development process, the contact geometry is integrated into the periodic pattern (step 4). This photoresist structure then again is used as a master structure in a cast moulding process to fabricate PDMS stamps for the actual NIL production process. In Fig. 4, SEM micrographs of the photolithographically patterned master structure [Fig. 4(b) show the result of the NIL process Fig. 4(c)] as well as the resulting texture in silicon after the plasma etching process and resist removal [Fig. 4(d)]. It can be seen that the contact finger geometry is successfully transferred into the texture in silicon. It is remarkable that the broader contact finger geometry is replicated by the NIL process with virtually no residual layer beneath it. This, in combination with the characteristics of the plasma etching process, leads to grooves for the latter metallization, which are even deeper than the honeycomb texture itself.

3.5 Fine Line Contact Fingers with Prismatic Profile

As discussed earlier, front contact fingers lead to shading effects and thus to optical losses. Therefore, techniques applied in the photovoltaic industry were constantly refined in order to realize narrower contact fingers preferably with

high aspect ratios. For screen-printed contact fingers, it was reported that not the full contact finger area leads to shading losses, but rather an effective shading area can be defined by considering parts of the contact finger where light is reflected onto the active cell area and not lost.²⁰ As a consequence of this thought, by a prismatic contact finger geometry, the effective shading can virtually be eliminated (neglecting reflection losses at the metal finger and the increased angle of incidence on the cell area).

In order to fabricate very fine contact fingers with a prismatic profile, a process chain was developed based on NIL, evaporation, and lift-off processes. For the master structure, v-grooves realized in silicon using photolithography and alkaline etching were used. PDMS stamps were replicated from these silicon masters and a NIL process was conducted using a bilayer resist system consisting of a Laromer PO84F resist from BASF, which is patterned by NIL, and a lift-off resist (LOR) layer beneath (MicroChem LOR10B). After the patterning of the imprint resist, the residual layer is opened using plasma etching; then, the LOR layer is opened in a development step (using AZ400K developer and deionized water in ratio 1:4). Next, the evaporation is conducted, where the sample is mounted in a way so that defined angles of the contact finger result. Finally, the lift-off process is conducted using the organic solvent N-Methyl-2-pyrrolidone (NMP). Figure 5 illustrates the different stages of this process chain, showing that the principle of realizing prismatic shapes and just 3- μm fine fingers was successfully demonstrated. However, it can be seen that an unwanted thin metal layer was deposited besides the contact finger. This effect results from an excessive opening of the LOR layer prior to the evaporation process. Thus, in a next step, the development of the LOR layer has to be optimized in order to eliminate this effect. Furthermore, the tip of the contact finger is not as sharp as it has been before the lift-off process. This can be attributed to the use of ultrasonic cleaning to promote the removal of the LOR layer. As a consequence, either the power has to be reduced or megasonic cleaning might be applied.

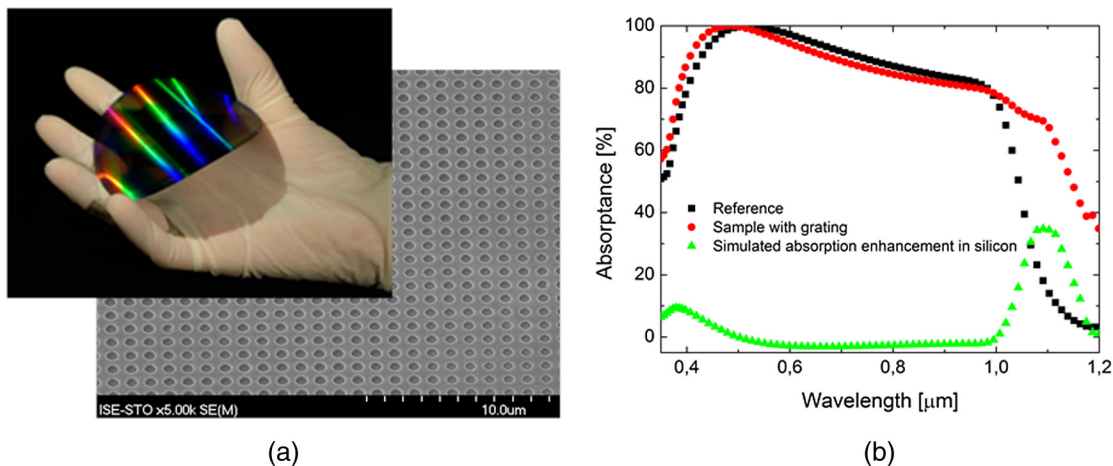


Fig. 3 (a) Photograph of an imprinted crossed grating with a pitch of 1 μm on a 50- μm -thick 4-in. monocrystalline silicon wafer. The bowing of the wafer highlights its flexibility. Also shown on the left side is an SEM micrograph showing the pattern in silicon after a plasma etching process. (b) Absorption measurements of a 200- μm -thick sample with such a rear side grating as well as of a planar reference are shown (including single-layer AR coating, dielectric buffer, and aluminum mirror on the rear). The simulated useable absorption enhancement in silicon is extracted from Ref. 18.

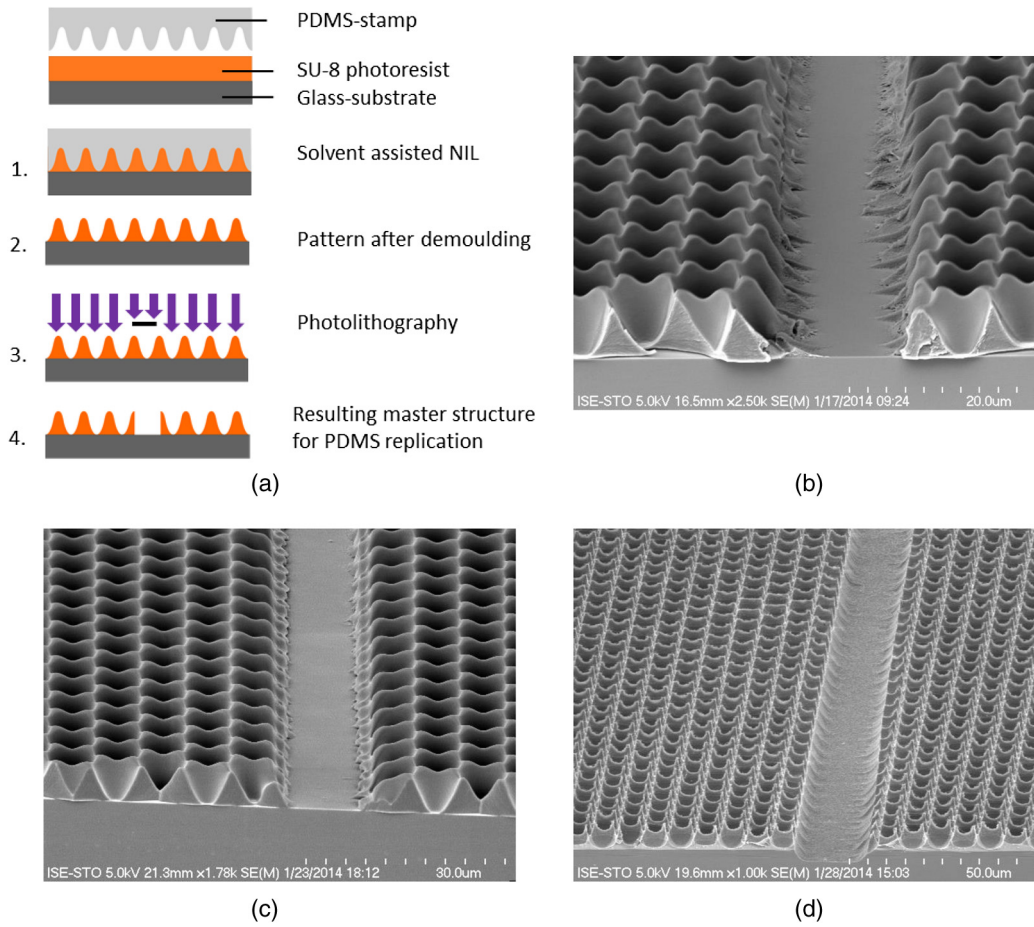


Fig. 4 (a) The process chain to integrate contact grid features into a pre-existing periodically patterned master structure is schematically visualized. (b) An SEM micrograph showing the resulting master structure (step 4) is given. (c) From this photoresist structure again, a polydimethylsiloxane (PDMS) mould is replicated and then used in a nanoimprint lithography (NIL) process. (d) The resulting texture after a plasma etching process is shown.

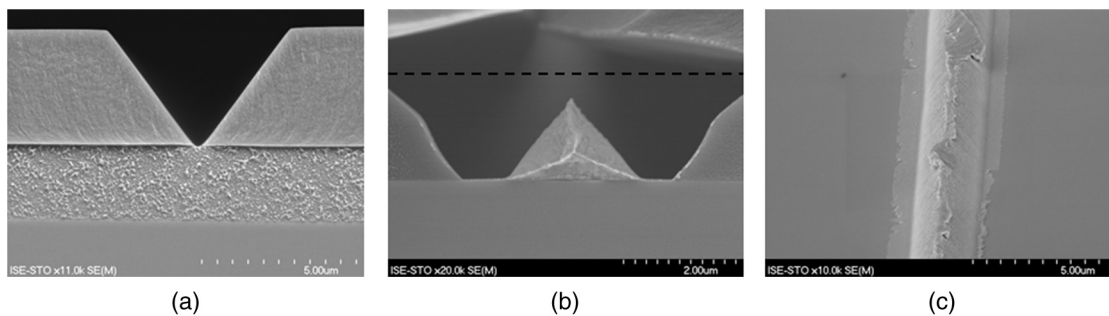


Fig. 5 (a) Bilayer resist system on a silicon substrate after the NIL process. Only the upper layer is patterned. (b) After a plasma etching and development step, silver is evaporated under defined angles leading to a prismatic metal finger, which is $2.5 \mu\text{m}$ broad and $1.6 \mu\text{m}$ high. (c) After the development process, an unwanted thin metal layer on both sides of the contact finger can be seen.

4 Summary and Outlook

This study investigates the application of nanoimprint lithography (NIL) for implementing defined textures in silicon solar cells using the SmartNIL process from EV Group. Honeycomb textures realized on large area multicrystalline silicon solar cells led to an enhancement of optical efficiency of 7% relative and a resulting total efficiency enhancement of 0.5% compared to the state-of-the-art texture based on

acidic wet chemical etching. This was achieved using high-throughput equipment for all other solar cell processing steps and an Al-BSF cell structure. As a result of superior internal reflection properties of solar cells with a passivated rear side cells (PERC cell structure), the optical gain is supposed to be even higher.

A more sophisticated approach to enhance light trapping in particular for very thin solar cells is based on the realization of

photonic features on the rear side of the solar cell. A very high absorption enhancement of up to 35% absolute at a wavelength of 1100 nm was demonstrated for 200- μm -thick wafers. This enhancement for long wavelengths is supposed to be even more pronounced for the very thin substrates. The study succeeded in realizing crossed grating patterns with a period of 1 μm on wafers of a thickness as low as 50 μm . Such rear side structures might also be very interesting in combination with standard micron-scale front side textures. Currently, the authors are working on a theoretical approach that allows to efficiently simulate combinations of textures in the range of several microns with ones lying in the wave optical regime and thus estimate the efficiency potential of such concepts.²¹

Furthermore, this study combined photolithography with NIL processes in order to integrate multiple features into the etching mask design. In this context, master structures containing periodic features for the honeycomb texturing as well as contact grid geometries were realized and these features were replicated via NIL and transferred into silicon using plasma etching. Such a structure might be used to realize buried contacts as described in Ref. 22. Benefits would be a reduced shading by the lateral delimitation of the contact finger area as well as a very defined contact formation due to the smooth surface.

As a final application, the paper presented the realization of very fine contact fingers with a prismatic shape in order to minimize shading effects of front contacts. Such prismatic fingers could in particular be interesting for multijunction PV approaches for reaching highest conversion efficiencies. Using this approach, the current efficiency record of 46% could be pushed even further.²³

Acknowledgments

Parts of this work were funded by the German Federal Ministry for Economic Affairs and Energy under Contract No. 0325292 (Fortes), the German Federal Ministry of Education and Research under Contract No. 03SF0401 (InfraVolt), and strategic funds of the Fraunhofer Gesellschaft. N. Tucher was supported by a grant from the Cusanuswerk, Bischöfliche Studienförderung, Germany which he gratefully acknowledges.

References

1. M. Peters et al., "Photonic concepts for solar cells," in *Physics of Nanostructured Solar Cells*, V. Badescu and M. Paulescu, Eds., pp. 1–41, Nova Science Publishers, Hauppauge, NY (2012).
2. F. Dross et al., "Crystalline thin-foil silicon solar cells: where crystalline quality meets thin-film processing," *Prog. Photovoltaics* **20**(6), 770–784 (2012).
3. M. Ernst et al., "Thin macroporous silicon heterojunction solar cells," *Phys. Status Solidi (RRL)–Rapid Res. Lett.* **6**(5), 187–189 (2012).
4. P. Campbell and M. A. Green, "Light trapping properties of pyramidally textured surfaces," *J. Appl. Phys.* **62**(1), 243–249 (1987).
5. A. Hauser et al., "A simplified process for isotropic texturing of mc-Si," in *Proceedings of 3rd World Conference on Photovoltaic Energy Conversion*, Vol. 2, pp. 1447–1450 (2003).
6. O. Schultz, S. W. Glunz, and G. Willeke, "Multicrystalline silicon solar cells exceeding 20% efficiency," *Prog. Photovoltaics* **12**(7), 553–558 (2004).
7. C. Heine and R. H. Morf, "Submicrometer gratings for solar energy applications," *Appl. Opt.* **34**(14), 2476 (1995).
8. International Technology Roadmap for Photovoltaic (ITRPV), Semi PV, 2014, <http://www.itrpv.net/Home/>
9. H. Hauser et al., "Honeycomb texturing of silicon via nanoimprint lithography for solar cell applications," *IEEE J. Photovoltaics* **2**(2), 114–122 (2012).
10. A. J. Wolf et al., "Origination of nano- and microstructures on large areas by interference lithography," *Microelectron. Eng.* **98**(0), 293–296 (2012).
11. B. Bläsi et al., "Photon management structures for solar cells," *Proc. SPIE* **8438**, 84380Q (2012).
12. A. Bietsch and B. Michel, "Conformal contact and pattern stability of stamps used for soft lithography," *J. Appl. Phys.* **88**(7), 4310–4319 (2000).
13. U. Plachetka et al., "Wafer scale patterning by soft UV-nanoimprint lithography," *Microelectron. Eng.* **73–74**, 167–171 (2004).
14. M. Muehlberger et al., "Nanoimprint lithography from CHARPAN Tool exposed master stamps with 12.5 nm hp," *Microelectron. Eng.* **88**(8), 2070–2073 (2011).
15. N. Tucher et al., "Crystalline silicon solar cells with enhanced light trapping via rear side diffraction grating," accepted for publication in *Energy Procedia* (2015).
16. P. Piechulla et al., "Increased ion energies for texturing in a high-throughput plasma tool," in *Proceedings at the 26th European Photovoltaic Energy Conference*, Hamburg (2011).
17. A. K. Volk et al., "Honeycomb structure on multi-crystalline silicon Al-BSF solar cell with 17.8% efficiency," *IEEE J. Photovoltaics* **99**, 1–7 (2015).
18. H. Hauser et al., "Diffraction backside structures via nanoimprint lithography," *Energy Procedia* **27**(0), 337–342 (2012).
19. A. Mellor et al., "Nanoimprinted diffraction gratings for crystalline silicon solar cells: implementation, characterization and simulation," *Opt. Express* **21**(S2), A295 (2013).
20. R. Woehl, M. Hörteis, and S. W. Glunz, "Analysis of the optical properties of screen-printed and aerosol-printed and plated fingers of silicon solar cells," *Adv. OptoElectron.* (2008).
21. J. Eisenlohr et al., "Matrix formalism for light propagation and absorption in textured optical sheets," *Opt. Express* **23**(11), A502 (2015).
22. J. C. Zolper et al., "16.7% efficient, laser textured, buried contact polycrystalline silicon solar cell," *Appl. Phys. Lett.* **55**(22), 2363–2365 (1989).
23. M. A. Green et al., "Solar cell efficiency tables (Version 45)," *Prog. Photovoltaics* **23**(1), 1–9 (2015).

Hubert Hauser studied microsystems engineering at the University of Freiburg with a focus on processes and materials. He received his PhD from the University of Freiburg for his work on "Nanoimprint Lithography for Solar Cell Texturisation" in 2013, which was realized at the Fraunhofer Institute for Solar Energy Systems (ISE). Since then he has worked as project manager in the microstructured surfaces group at Fraunhofer ISE.

Biographies for the other authors are not available.